

Developing Beach Litter Monitoring System Based on Reflectance Characteristics and its Abundance

I Made Oka Guna Antara^{1,2*}, I Wayan Nuarsa¹, I Made Sudarma¹,
I Gede Hendrawan¹, Muhammad Reza Cordova³

¹ Doctor Study Program of Environmental Science, Graduate Program, Universitas Udayana, Jalan P.B. Sudirman, Denpasar, Bali 80232, Indonesia

² Research Center for Environmental, The Institute of Research and Community Services, Universitas Udayana, Jalan P.B. Sudirman, Denpasar, Bali 80232, Indonesia

³ Research Center for Oceanography, The Indonesian National Research and Innovation Agency (BRIN), BRIN Kawasan Jakarta Ancol Jalan Pasir Putih 1, Ancol Timur, Jakarta 14430, Indonesia

* Corresponding author's e-mail: oka@unud.ac.id

ABSTRACT

Marine litter is a major global problem; it originates on land and enters the ocean via rivers, coastal erosion, and extreme events. Over time, marine litter collects in coastal areas. As a result, the research on litter dispersal and buildup is critical for successful coastal area management. Addressing the knowledge gap is critical for establishing successful solutions to fight that problem. In recent years, a variety of remote sensing techniques have been used to better understand litter abundance, distribution patterns, and dynamics in marine as well as coastal ecosystems. Marine litter detection and quantification are carried out using aircraft-based imaging systems, satellite images, and unmanned aerial vehicles (UAVs). The purpose of this study was to create a beach litter monitoring system or technical reference using a small UAV and geographic information system (GIS), with the test location at Batu Belig Beach, Badung Regency, Bali, Indonesia. The box-plot approach was used to determine the reflectance threshold on the orthophoto. GIS is used to determine the regions with and without litter based on the set threshold values. To verify the model, Slovin's Formula was used to collect the sample, with a confusion matrix indicating an accuracy of 80%. This monitoring system provides a simple approach for identifying and measuring litter, even with only one person handling the entire operation. The outcomes of this analysis indicated that the majority of litter at the study location was made up of white plastic bags and styrofoam. As a last step, portraying litter abundance as a percentage per square meter was considered.

Keywords: remote sensing, GIS, UAV, beach litter, box-plot method.

INTRODUCTION

Indonesia is a nation heavily dependent on its oceans for development and global integration (Rochwulaningsih et al., 2019), it also serves as an important reservoir of biodiversity (Gunawan et al., 2022). However, this unique relationship is now at risk due to the detrimental impact of human activities such as marine litter. As one of the top five contributors to plastic waste in global oceans, Indonesia faces significant threats to its coastal and marine ecosystems (Cordova et al.,

2022; Cordova and Nurhati 2019; Lebreton et al., 2012; Lestari and Trihadiningrum 2019; Phelan et al., 2020; Sakti et al., 2023; van Emmerik Schwarz 2020). Marine litter can significantly impact economic stability because of the adverse perception, especially in the marine tourism destination (Grelaud and Ziveri 2020).

In Indonesia, the economy of the Bali Province depends on tourism destinations (culture and ecology), one of which is marine tourism; nowadays, it is particularly susceptible to the dangers posed by marine debris (CNN Indonesia, 2021;

Hajar, 2019; Mauludy et al., 2019; Suteja et al., 2021). The presence of such debris jeopardizes various variables within these invaluable ecosystems. On the basis of the data from the Indonesian Ministry of Environment and Forestry (2020), Indonesia generates approximately 13 million tons of unmanaged waste per year, with plastic accounting for the second highest proportion (17.10%) after food waste. In the Bali Province alone, daily waste generation amounts to 4,281 tons or an annual total of 1.5 million tons (Muhajir 2019).

Marine litter is a major issue in coastal and marine ecologies, and it is currently a significant concern in our society (Gonçalves et al., 2022). Marine litter originates from land and enters the ocean through rivers, coastal erosion, and extreme events (Cordova et al., 2022; Geraeds et al., 2019; González-Fernández and Hanke, 2017; Liro et al., 2020; Maharjan et al., 2022; Meijer et al., 2021; Sakti et al., 2023; van Emmerik, Roebroek, et al., 2020; van Emmerik, Seibert, et al., 2020; van Lieshout et al., 2020; Vriend et al., 2020). Over time, a substantial amount of this litter accumulates on beaches, which is a risk and possible adverse effects (Pinto et al., 2021). Several studies reported on the adverse effects of marine litter to environments, marine biota and human blood (Argeswara et al., 2021; Lam et al., 2022; Leslie et al., 2022). Thus, it is crucial to study the litter distribution, accumulation and its abundance; it can be used to effectively manage coastal areas affected by marine litter (García-Rivera et al., 2018; Merlino et al., 2020; Miladinova et al., 2020).

Various studies have been conducted on the topic of coastal and marine litter, focusing on aspects such as the types, quantities, distribution, and sources of these pollutants. Traditionally, researchers have relied on the methods involving data recording and statistical sampling to investigate beach litter by going to the location (Cordova and Nurhati 2019; Hardesty et al., 2021; Schuyler et al., 2020; Secretariat of the Convention on Biological Diversity, 2016). However they are costly, time-consuming, and require many people (Merlino et al., 2020; Schuyler et al., 2020).

In recent years, remote sensing techniques have been utilized to enhance the understanding of litter abundance, distribution patterns, and dynamics in marine and coastal environments. These techniques include balloon- and aircraft-based imaging systems as well as satellite imagery that enables the detection and quantification of litter worldwide (Cózar et al., 2021; Freitas et al., 2021;

Garcia-Garin et al., 2021; Goddijn-Murphy et al., 2018; Kako et al., 2012; Kikaki et al., 2020; Maximenko et al., 2019; Serafino and Bianco 2021; Topouzelis et al., 2020). The use of Unmanned Aerial Vehicles (UAV) has significantly increased for environmental monitoring purposes. These autonomous aerial platforms have proven to be effective tools for identifying and quantifying litter in coastal environments. Their ability provides high-resolution images and affordability, UAV offer a viable solution for conducting operational macro-litter (>2.5 cm) surveys across various ecosystems, including beach areas (Andriolo et al., 2020, 2021, 2022; Bak et al., 2019; Bao et al., 2018; Garcia-Garin et al., 2021; Geraeds et al., 2019; Goddijn-Murphy et al., 2022; Martin et al., 2018; Merlino et al., 2021, 2020; Topouzelis et al., 2019, 2020).

However, the utilization of UAV for monitoring beach litter has yet to be widely documented in the research literature, especially in Indonesia. UAVs are equipped with radio remote-control devices and programmable control systems that allow them to operate autonomously or under computer guidance. These advanced systems produce high-resolution products with precise measurements using cost-effective cameras (Mandirola et al., 2021; Xiao et al., 2022).

Addressing the knowledge gap regarding marine litter is crucial for developing effective strategies to combat this problem. Insufficient information hinders the understanding of potential ecological impacts, such as changes in species composition due to litter. By identifying the areas with high concentrations of marine litter, its effects can be better predicted and preventative measures can be taken against land-based leakage (González et al., 2016; Haseler et al., 2018; Veiga et al., 2016). This study investigated the use of low-cost UAV technology for studying and identifying marine litter on beaches. The aim was to provide a technical reference, including threshold values, for monitoring beach litter. Through this work, it is sought to increase the utilization of affordable UAVs in enhancing the understanding of litter quantity, composition, and changes along coastlines.

MATERIALS AND METHODS

Brief description of study location

The location of study is situated at Batu Belig Beach in the Badung Regency area of Bali,

Indonesia (8.6742447°S and 115.1459553°W, Figure 1). This beach, located on the shore of the Indian Ocean and facing directly towards the Bali Strait, is a sandy beach with minimal gravel and pebble content. Numerous studies have indicated that there is an accumulation of litter on this stretch of beach throughout the year, particularly during the west monsoon season from December to April. The litter originates from both land-based sources as well as anthropogenic activities associated with sea-based sources. According to the estimates provided by Bali Partnership (2019), approximately 3000 kg/day to 6000 kg/day of litter flows out from nearby rivers into the vicinity of the Batu Belig Beach, which poses potential hazards for this study area.

Experimental design

The flowchart illustrating the experimental design is presented in Figure 2. The aim of this study was to develop a streamlined system that can be effectively implemented by one person, minimizing resource requirements from preparation to data visualization. The experimental design encompasses four stages: planning and executing UAV missions; processing UAV images; conducting post-image analysis; and

validating results and generating maps depicting litter abundance.

UAV mission planning

This study utilized a DJI Mavic 2 Pro, a commercial drone equipped with 1” 20-megapixel CMOS camera sensor and 77° FOV (<https://www.dji.com/mavic-2>). The drone was operated through the DJI Go 4 apps on an iPhone XR, using dronelink mission planner software available on IOS and android (<https://www.dronelink.com/>) to scan specific areas autonomously. Prior to this, the Area of Interest (AoI) was defined using QGIS 3.28.5-Firenze, its purpose is to obtain an accurate and specific location. A series of photographs were captured under various operational conditions, as mentioned earlier. The camera was consistently positioned to investigate the ground at a 90° angle with automatic settings. To achieve photo alignment, the UAV speed was adjusted at different altitudes to ensure an overlap of more than 70% between each successive photo and the previous one. The resolution of the orthoimage photos was determined to be less than 2.5 cm/pixel when taken at an altitude of 60 meters above ground level. The extent of the experimental area surveyed by the UAV varied depending on its altitude and spanned approximately

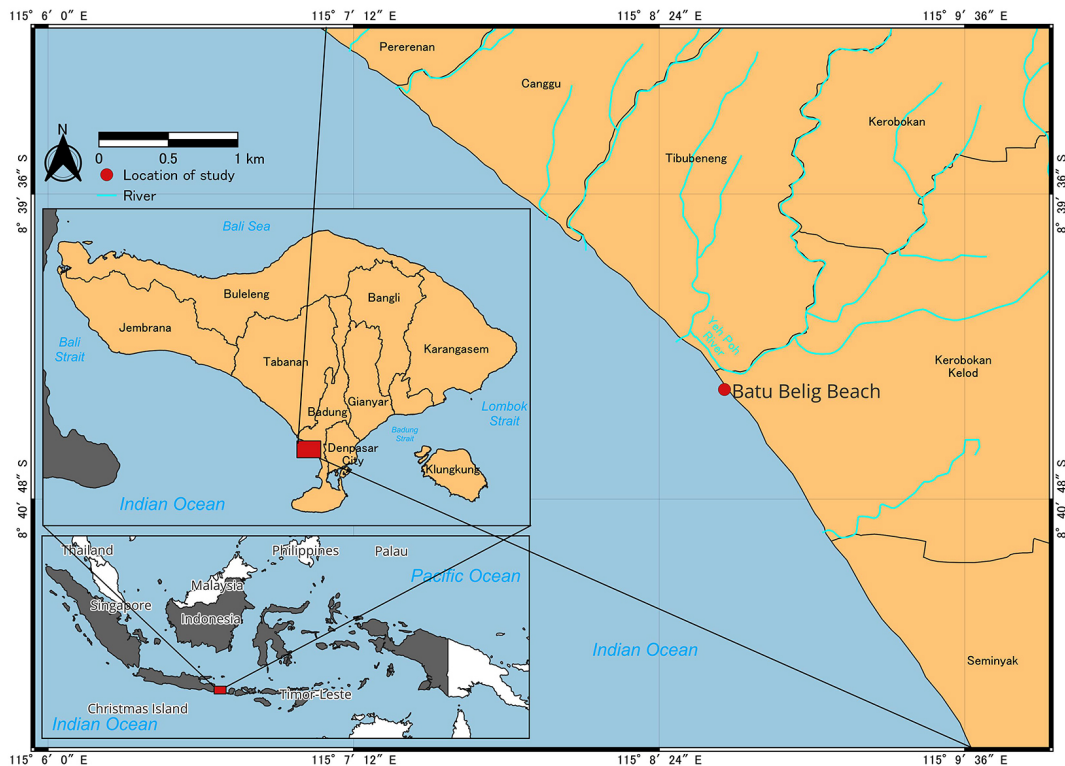


Figure 1. Location of study

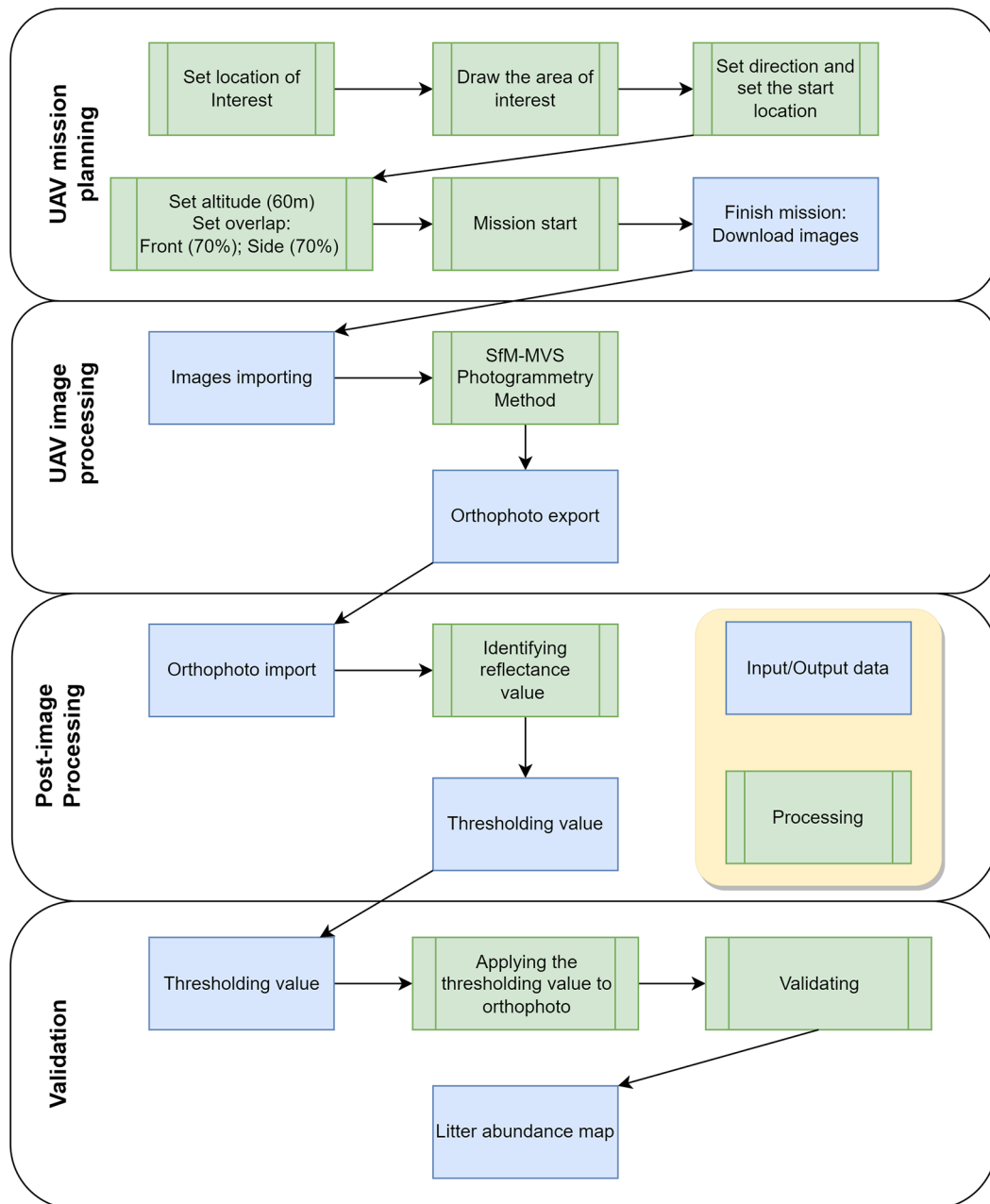


Figure 2. Experimental design flowchart

300 meters. The relations between altitude with the pixel size resolution is given by Ground Sample Distance (GSD) shown in Eq. 1 (Aber et al., 2019).

$$GSD = \left(\frac{\text{Sensor width in mm}}{\text{image width in pixel}} \right) \times H_g / f \quad (1)$$

where: H_g – altitude or average height above the ground in meter and f – the lens focal length of camera in mm.

UAV image processing

Immediately, the images taken were automatically aligned to generate an orthophoto

using SfM-MVS photogrammetry method and by QGIS 3.28.5-Firenze for post-image processing and analyzing. The SfM-MVS photogrammetry method follows the workflow proposed by Over et al. (2021).

Post-image processing

Subsequently, the orthophoto undergo post-processing through an analysis of reflectance image values using a box-plot method. This approach involves creating a visual representation of the data distribution without imposing any limitations. The box plot technique has been

commonly utilized to identify quartile and inter-quartile ranges, as well as outliers in data sets. Quartile ranges provide insights into centrality, dispersion, and shape of the data distribution. Outliers can be identified using boxplot analysis, shown in Eq. 2 (Wang et al., 2023).

$$V_0 = \begin{cases} QL - 1.5 \times IQR \text{ or } T_0 \\ QU + 1.5 \times IQR \text{ or } T_1 \end{cases} \quad (2)$$

where: V_0 denotes the edge of the outlier, QL denote the lower (25th percentile) and QU denote the upper (75th percentile) quartiles, which indicate that 25% of all observations have data values that are below or above the corresponding quartile values, respectively, and IQR denotes the interquartile range between QL and QU , which covers 50% of observations. The T_0 and T_1 is minimum and maximum threshold, respectively. If no has fliers in the box-plot, T_0 is equal to the min value and T_1 is equal to the max value.

Validation

To determine the sample for validation, Slovin's Formula with confidence level 85% and confidence interval 15% is used, the formula shown in Eq. 3 (Mandal and Dey, 2022).

$$n = N / (1 + Ne^2) \quad (3)$$

where: n – number of samples, N – total population (total litter calculated in attribute table QGIS software), e – error tolerance (level).

The validation process involves the use of a confusion matrix, where orthophoto is utilized as the validating images. The confusion matrix (as depicted in Figure 3) represents the validating classes on the y-axis and the prediction classes on x-axis. True Positive is used to denote the correctly predicted litter classes, while False Negative refers to the valid litter that was incorrectly predicted as no litter. Similarly, true negative indicates correctly predicted no litter, whereas False Positive signifies the instances where litter was classified erroneously. These values can be employed for various statistical measurements including precision, recall, f_1 score, and accuracy (Papakonstantinou et al., 2021).

The calculation for precision is provided in Eq. 4 (Papakonstantinou et al., 2021), which is

the proportion of correctly predicted litter to the total number of litters. On the other hand, recall is defined as a metric that represents the percentage of accurately classified predictions out of all detected litter instances shown in Eq. 5 (Papakonstantinou et al., 2021).

$$Precision = \frac{TP}{TP+FP} \quad (4)$$

$$Recall = \frac{TP}{TP+FN} \quad (5)$$

Nevertheless, when dealing with imbalanced datasets, both methods have limitations in accurately assessing the models' performance. Therefore, it is necessary to combine them into a single statistical calculation known as the harmonic mean value or f_1 score (Eq. 6) (Papakonstantinou et al., 2021). The accuracy of identifying tiles throughout the entire dataset can be measured using Eq. 7 (Papakonstantinou et al., 2021).

$$f_1 \text{ score} = \frac{2 \times Precision \times Recall}{Precision + Recall} \quad (6)$$

$$Accuracy = \frac{TP+TN}{TP+TN+FN+FP} \quad (7)$$

The last processing is generated litter coverage map by using grid 5×5 m or 25 m^2 , using the equation shown in Eq. 8 is proposed.

$$A_L = A_T - A_{nL} \quad (8)$$

where: A_L – litter coverage in area [m^2], A_T – total area/grid 5×5 m or 25 m^2 [m^2], A_{nL} – area with no litter coverage [m^2].

Validating	litter	TP	FP
	no_litter	FN	TN
		litter	no_litter
		Prediction	

Figure 3. The illustration of confusion matrix (Papakonstantinou et al., 2021)

RESULTS AND DISCUSSION

UAV mission and orthophoto results

This study is the first instance of conducting a comprehensive experimental design at Batu Belig Beach in Bali, Indonesia by integration of the UAV missions and Geographic Information Systems (GIS) approaches with a thresholding method. Traditionally, researchers have utilized data collection and statistical sampling techniques to examine beach litter (Cordova and Nurhati 2019; Hardesty et al., 2021; Schuyler et al., 2020; Secretariat of the Convention on Biological Diversity, 2016). However, these previous methodologies are both costly and time-consuming, as they require personnel to physically visit the location for data collection using line transects (Merlino et al., 2020; Schuyler et al., 2020). Typically, three lines are drawn from the boundaries affected by waves to the boundaries between sand and land (such as scrub or buildings) at each location. This method requires 3–5 people who spend around 40–50 minutes per location depending on their proficiency and experience level (Schuyler et al., 2020). Furthermore, the previous approach lacks repetitive spatial and temporal coverage. In terms of classification, it heavily relies on personnel judgment based on their expertise and experience (Andriolo et al., 2021; Merlino et al., 2021). Another issue is accessibility; often, monitoring locations are difficult to reach and pose potential safety hazards (Yang et al., 2022).

To address these challenges in beach litter monitoring, this methodology that leverages low-cost commercial UAV integrated with GIS is proposed (Jakovljevic et al., 2020; Lo et al., 2020). In contrast to the adopted approach, they have developed a methodology for this study that offers several advantages. Firstly, it significantly reduces costs in repeatable use and time consumption by allowing the data collection to be carried out by just one person. This method also allows for spatiotemporal repetition and enables the study of larger areas of interest. In terms of data processing, it has implemented a simplified approach using threshold reflectance values along with the assistance of box-plot analysis. The aim was to make the data processing as easy and efficient as possible, even for researchers without extensive knowledge in this area.

The UAV type used was a DJI Mavic 2 Pro, with Global Positioning System (GPS) and Global

Navigation Satellite System (GLONASS); thus, this UAV allows communicating with several existing satellite communications. This is related to the coordinates produced accuracy on orthophoto. This mission is conducted without Ground Control Points (GCP), however orthophoto result has the required quality. It will improve the efficiency of time and human resources, and repetition observations. Repetition observations are important in determining abundance characteristics over the time (Haseler et al., 2018). The mission was carried out on April 11th, 2023, at 12.20 PM Central Indonesian Times (WITA), with fair weather condition and a wind speed of 6.70 m/s from the west. During this study, the season is the transition from rainy to dry season, 1 (one) hour before the mission start, there was drizzling rain.

The flight altitude was set at 60 m above ground level, this is because of the location characteristics. Previous studies used lower altitudes, Gonçalves et al. (2020) carried out studies at 20 m above sea level. Batu Belig Beach is an area with many tourist attractions and accommodations. Here, there are tall trees, such as coconut trees, like normal beaches in tropical areas. The result of orthophoto is shown in Figure 4, with pixel size ~1.35 cm/pixel is produced. This pixel size can capture beach litter objects with more than 2.5 cm, as shown in Figure 5. A macro litter shape can be represented with a minimum of 4×4 pixels (approximately 2.71 cm) on Figure 5 displays a comparison between litter capture at altitudes of 6 m (Figure 5a) and 60 m (Figure 5b), using a size reference of 22 cm². On the basis of the experiment, it provides advantages in the form of observation speed (1.8 ha in 6 minutes 38 seconds) and safety in the areas containing higher trees.

Data and accuracy analysis

The data processing finished in less than 60 minutes, starts with extracting Digital Number (DN) on pixel scale, filtering DN to get threshold value, binary classification (applied thresholding method), and calculating covering area by litter abundance. In advance of thresholding analysis, visual screening on orthophoto is conducted. The obtained findings are not grouped into the material sources but based on its color, because the UAV used was a small-UAV with normal RGB-camera, like mentioned in section UAV mission planning. However, plastic litter are grouped into 8 different litter categories (Figure 6), i.e. another object



Figure 4. Orthophoto of the area of interest at 60 m altitude

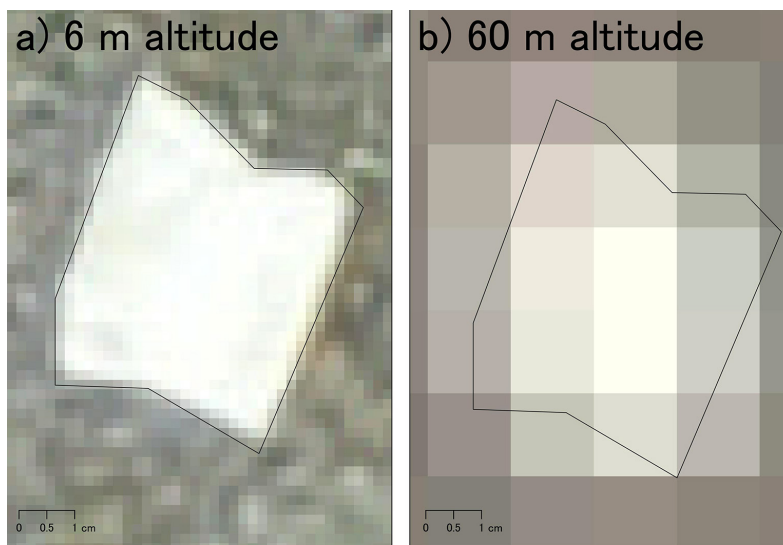


Figure 5. Litter with size 22 cm²: (a) 6 m altitude and (b) 60 m altitude

with blue color (Figure 6a); plastic bag with black color (Figure 6b); plastic bag with blue color (Figure 6c); plastic bag with green color (Figure 6d); plastic bag with red color (Figure 6e); plastic bag with transparent color (Figure 6f); plastic bag with white color (Figure 6g); and Styrofoam (Figure 6h). Most of them are white plastic bags and Styrofoam. These findings are interesting in investigating the sources, especially Styrofoam. Compared to Suteja et al. (2021), who conducted their manual investigation at the near location (Petitenget and Legian Beach) of Batu Belig Beach at 2021, the most of litter is plastic, both in rainy and dry season. In this location, the authors found the unique organic litter dumping which originates from cultural activities (ceremonial facilities) and results of peeling coconut by local people, shown in Figure 7. In fact, litter dumping can only be found in the Bali Areas. Contrasting

to Cordova and Nurhati (2019) at Jakarta Bay, they did not found it, which is due to the differences of culture root even though the study was also conducted in Indonesia. On this beach, by visual observation during this experiment, the litter stranded is dominated by organic matter including wood and leaves, which is because of its location near the Yeh Poh River mouth and transported from upstream.

Then, by using “Point Sampling Tools” QGIS 3.28.5-Firenze, each sample (Figure 6) is extracted to obtain the DN of reflectance value including sand (as a limitation). In order to obtaining the threshold value based on the DN reflectance value, the box-plot method is developed by Python code (<https://github.com/madeoka/BoxPlot>), the result is shown in Figure 8 for the box-plot figure and its statistics are shown in Table 1, 2, and 3 for red, green and blue band, respectively.



Figure 6. Points sampling profile in each category: (a) another object with blue color; (b) plastic bag with black color, (c) plastic bag with blue color, (d) plastic bag with green color, (e) plastic bag with red color, (f) plastic bag with transparent color, (g) plastic bag with white color, (h) styrofoam, (i) sand

Figure 8 shows the DN value characteristics or profile of red, green, and blue bands for each sample or objects. Figure 8a shows the profile of another object with a blue color; blue band has a higher value, reaching DN is equal to 255, whereas red and green band are lower than that. It is related to the color profile of the object. Figure 8b shows the profile of plastic bag with black

color; due to this object having black color, the value of RGB bands is lower and approaches zero. However, that profile does not attain the perfect zero value; this occurs because the objects on the orthophoto are mixed with another color especially white color from sunlight emitted. Figure 8c shows the profile of plastic bag with blue color; this was classified as plastic bag, rather



Figure 7. Organic dumping by local activities

Table 1. Red band reflectance values analysis by box-plot method

Object name	Statistical summary								
	Red Band (DN)								
	Min	Mean	Max	T_0	Q1	Median	Q3	T_1	IQR
Another object with blue color	7	97	212		63	90	132		69
Plastic bag with black color	26	70	155		52	62	87	140	36
Plastic bag with blue color	0	62	191		21	56	102		81
Plastic bag with green color	22	127	218		76	131	174		98
Plastic bag with red color	106	199	250	131	186	208	223		37
Plastic bag with transparent color	60	168	214	104	154	176	188		34
Plastic bag with white color	187	225	249	189	216	229	234		18
Styrofoam	120	236	255	185	227	251	255		28
Sand	84	133	179	86	122	135	146		24

Table 2. Green band reflectance values analysis by box-plot method

Object name	Statistical summary								
	Green Band (DN)								
	Min	Mean	Max	T_0	Q1	Median	Q3	T_1	IQR
Another object with blue color	89	172	226	127	160	171	182	206	22
Plastic bag with black color	28	67	147		48	58	82	133	34
Plastic bag with blue color	108	183	255		152	183	203		51
Plastic bag with green color	90	173	248		129	180	211		82
Plastic bag with red color	45	117	211		88	113	134	203	46
Plastic bag with transparent color	115	182	230	130	169	185	195		26
Plastic bag with white color	185	228	254	191	219	232	238		19
Styrofoam	113	237	255	208	236	252	255		19
Sand	83	128	173		117	129	141		24

Table 3. Blue band reflectance values analysis by box-plot method

Object name	Statistical summary								
	Blue Band (DN)								
	Min	Mean	Max	T_0	Q1	Median	Q3	T_1	IQR
Another object with blue color	103	199	255	117	178	201	219		41
Plastic bag with black color	31	70	140		53	64	85	132	32
Plastic bag with blue color	116	175	255		149	171	192		43
Plastic bag with green color	60	141	205		112	137	170		59
Plastic bag with red color	35	128	225		98	122	157		59
Plastic bag with transparent color	108	179	224	134	168	183	191		23
Plastic bag with white color	195	232	253		224	236	243		20
Styrofoam	102	236	255	225	241	247	252		11
Sand	89	125	167		115	124	135	165	20

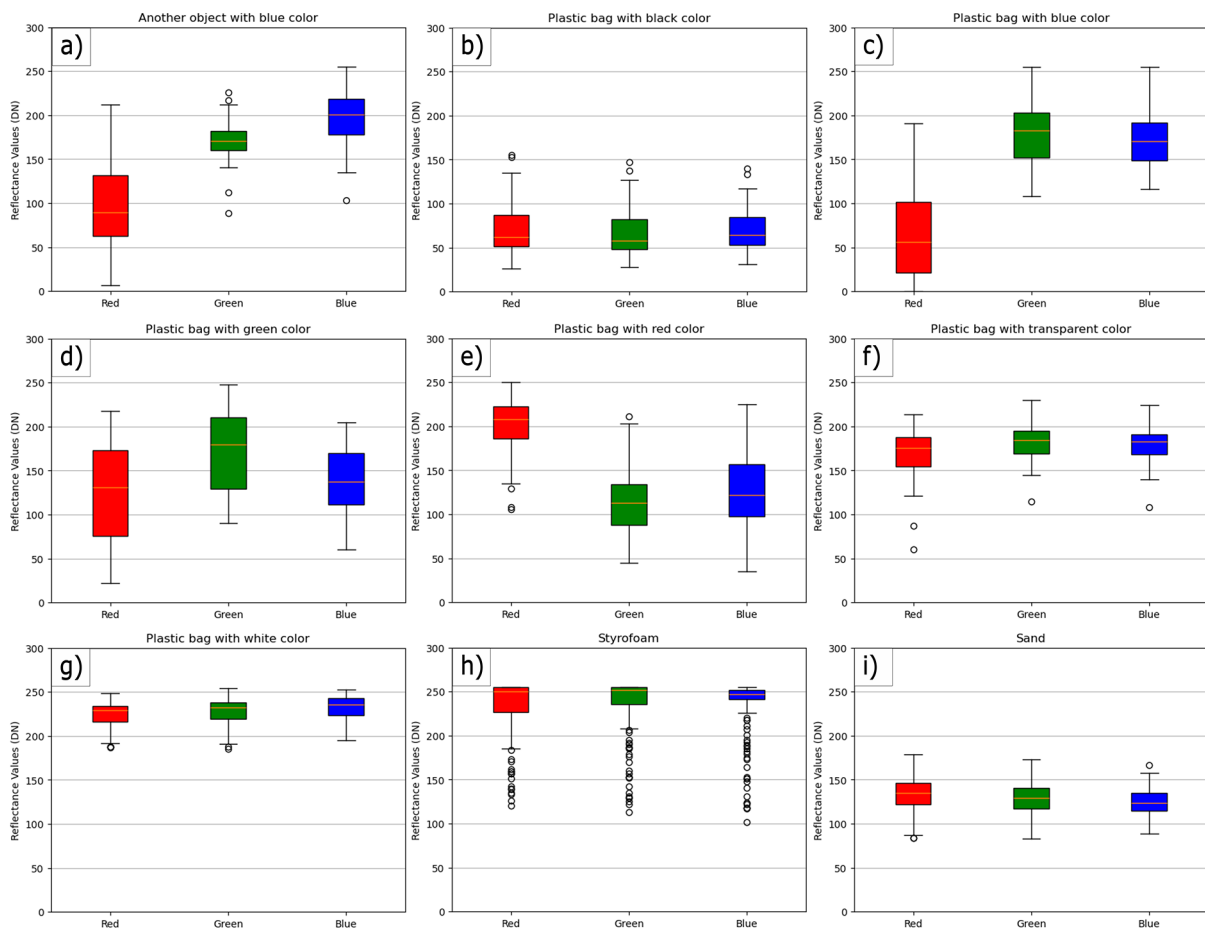


Figure 8. The box-plot summaries of the point sampling profile in each category from Figure 6. (a) another object with blue color, (b) plastic bag with black color, (c) plastic bag with blue color, (d) plastic bag with green color, (e) plastic bag with red color, (f) plastic bag with transparent color, (g) plastic bag with white color, (h) styrofoam, and (i) sand

than another object with blue color (Figure 8a) based on its shape and color. Then, the authors obtained the profile with blue and green bands are higher DN values, reaching 255, where the red

band is lower than both bands. blue and green bands are reaching 255 because the object color is mixed between blue and green color, close to ocean green color (RGB: 72, 191, 145). Figure 8d

shows a plastic bag with green color; because the color is green, so this object is dominant in green band (DN=248) and other bands are lower. Figure 8e shows a plastic bag with red color profile; of course, the dominant band is red band (DN=250), and other bands are lower. Figure 8f shows a plastic bag with transparent color profile; because of these objects are transparent, the DN values are disturbed by background such as sand or other litter. The obtained finding shows the median of color profiles for each band are 176, 185, and 183 (R, G, and B). Figure 8g shows the profile of plastic bag with white color; theoretically in RGB composite white color is formed by RGB band with value 255. However, the value of each DN does not reach 255, the value is 249, 254 and 253 for R, G, and B respectively. Its value is disturbed by its shadow, this is related to the plastic texture which is not flat. Next is the most interesting object to pay attention to, namely styrofoam, shown in Figure 8h. This object has higher value compared to other objects with DN equal to 255 for all bands. The higher values are related to the perfect reflection by the object because the Styrofoam material characteristic in this location is flat shape. Figure 8i shows the profile of sand, the DN values have interval 86–179, 83–173, and 89–165 for red, green and blue band, respectively. Thus, some samples require cutting or excluding their interval values by sand to clearly establish threshold value. Therefore, after excluding DN from sand, the threshold for each sample (Tables 1, 2, and 3) are generated into Table 4 in using T_0 and T_1 as minimum and maximum threshold values, respectively. If there are no values of T_0 and T_1 , the authors used T_0 from min and T_1 from max as values mentioned in Eq. 2. Table 1 shows the red band

statistical value with the maximum value of styrofoam (DN=255) and the minimum value is plastic bag with blue color (DN = 0). It means styrofoam has perfect reflectance, as mentioned above and plastic bag with blue color does not have red band characteristics or influence. Table 2 shows the green band statistical value, the maximum value also by styrofoam (DN = 255) and same reason as Table 1, while the minimum value is plastic bag with black color (DN = 28). The last is Table 3, which shows blue band statistical value, the maximum value is from styrofoam, so the authors could draw the conclusion that styrofoam has a perfect reflectance value and is near white color (R, G, B = 255, 255, 225), while the minimum value giving by plastic bag with black color. As mentioned in Tables 2 and 3, a plastic bag with black color has a minimum value because that is equal to black (R, G, B = 0, 0, 0), while this value does not attain the perfect value to black, because the shape of an object and its disturbance by sunlight. Fortunately, two categories of litter which is the most litter do not need to be excluded. Therefore, the blue band was selected in this study due to its wide range of values from 165 to 255. Table 4 shows the threshold reflectance values after excluding DN value of sand (lower than 165 for blue band).

Figure 9 shows the experiment by using threshold selected was applied in using binary classification. Figure 9a depicts the clipping area determined through processing in the blue band, while Figure 9b displays the results obtained through grid-based thresholding. In Figure 9b, the selected grid locations for validation were shown with blue color rectangle (6 locations), chosen randomly using the “Random selection” command available in QGIS 3.28.5-Firenze. The

Table 4. The threshold reflectance values

Object	Reflectance value (DN)					
	Red		Green		Blue	
	T0	T1	T0	T1	T0	T1
Another object with blue color	179	255	173	255	165	255
Plastic bag with black color	179	255	173	255	165	255
Plastic bag with blue color	179	255	173	255	165	255
Plastic bag with green color	179	255	173	255	165	255
Plastic bag with red color	179	255	173	255	165	255
Plastic bag with transparent color	179	255	173	255	165	255
Plastic bag with white color	189	255	190.5	255	195	255
Styrofoam	185	255	207.5	255	224.5	255
Sand (excluded)	0	179	0	173	0	165

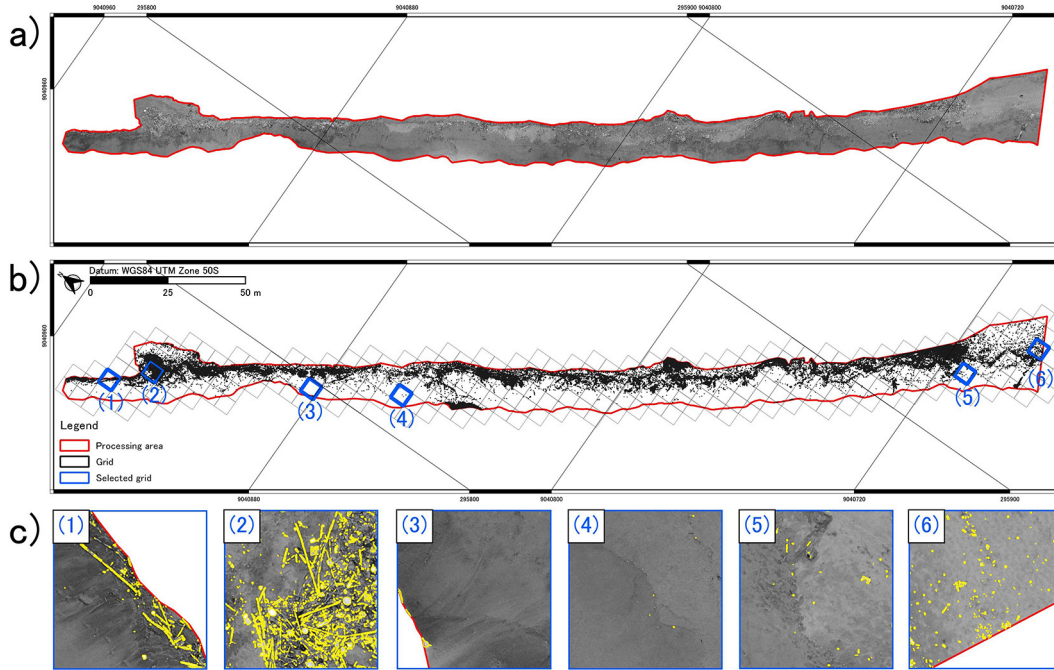


Figure 9. Experimental result: (a) clipping location by processing area in blue band; (b) result by applying the thresholding method with grid; (c) zooming grid selection

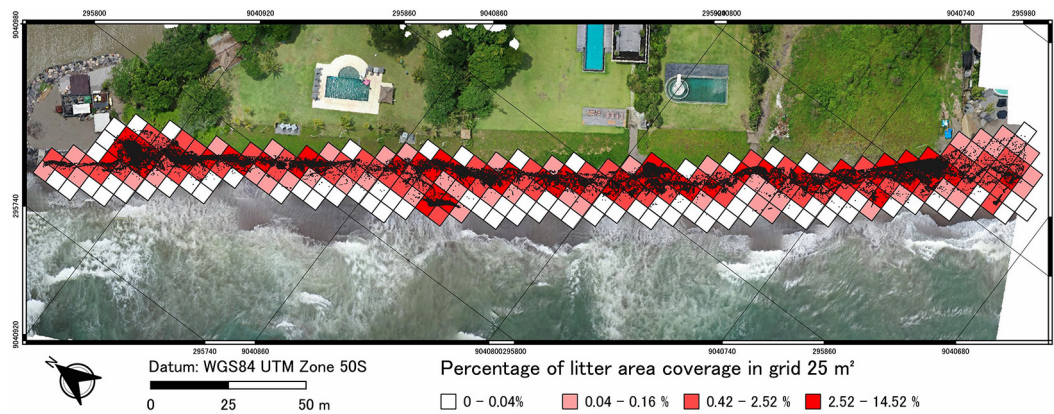


Figure 10. Map of percentage of litter area coverage in grid 25 m²

zoomed-in views are displayed in Figure 9c based on the grid location for validation.

In evaluation, the Slovin’s formula was applied to calculate the required number of samples, yielding a result of 44.4 (rounded to 44) samples for a total population of 43, 435-pixel groups representing litter. Subsequently, these samples were distributed across a grid measuring 5×5 m consisting of 252 grids shown in Figure 8b. By dividing the total number of grids by the number of samples, it was determined that each sample would cover approximately 5.6 (rounded up to 6) per grid. Same as grid selection, sample selection was random using the “Random selection” command. The validity of the obtained results was assessed

using a confusion matrix, the calculated outcomes of which are depicted in Table 5. The obtained findings demonstrate a precision rate of 85%, 95% recall rate, 89% f_1 -score value, and 80% of overall accuracy score. As mentioned in Table 4, the threshold range for detection is set between values ranging from 165 to 255 while taking into consideration the exclusion of sand. These methods prove to be effective specifically when identifying plastic bags with white color and Styrofoam, as these tend to be the most prevalent types of litter found within this location. It should be noted, the validation results did not yield any true negative predictions, meaning no instances where actual litter was correctly identified as non-litter items.

Table 5. Matric accuracy

Matric	Value
TP	34
FP	6
FN	3
TN	0
Precision	0.85
Recall	0.92
f_1 score	0.89
Accuracy	0.80

Monitoring results and discussion

The final outcome culminates in the production of a visualization the distribution of litter coverage across a grid size of 25 m². That monitoring result is presented in Figure 10, wherein varying shades ranging from white to red depict an ascending progression in the percentage value indicative of litter coverage area. Specifically, this scale ranges from 0% up to 14.52%, corresponding to an actual measurement encompassing a range between 0 m² and approximately 3.63 m² (in 100% is 25 m²). Compared to Bao et al. (2018) and Papakonstantinou et al. (2021), the litter abundance map by using 25 m²- grid with overlapping the result of thresholding method has been proposed in this research given the stranded patterns, range, location, litter coverage and possibility sources of litter more clearly. In order to compare with traditional sampling method (Cordova and Nurhati 2019; Hardesty et al., 2021; Schuyler et al., 2020; Secretariat of the Convention on Biological Diversity, 2016), this method provides more specific litter location information but is limited to litter characteristic types.

The adopted experiment methodologies are slightly different from the approach taken by Bao et al. (2018) in terms of assist of box-plot method. Contrasting with the new method in adopting artificial intelligence (Anadkat et al., 2019; Conley et al., 2022; Gonçalves et al., 2020; Kraft et al., 2021; Kylili et al., 2019; Martin et al., 2018; Nazerdeylami et al., 2021; Papakonstantinou et al., 2021; Pinto et al., 2021; Wolf et al., 2020), the method adopted by the authors is friendly in using thresholding method. It is because it is easy and faster to adapt to different locations, with no requirement for complicated new training data if has different litter characteristics. Another advantage of this method compared to the latest

method, i.e. artificial intelligence, is in area coverage. It only uses object classification without measuring the shape of litter abundance. Last but not least, the thresholding method does not require operators with strong data analysis (Bao et al., 2018) and processing knowledge with minimal effort and fault possibility. Once again, binary classification of litter and non-litter by threshold value, it is done by “raster calculator” in QGIS 3.28.5-Firenze and the last task is calculating the percentage of coverage area covered by litter. No less important is that in data processing, high PC computation is not needed.

However, this method has limitations, one corresponds to the reflectance value interval, which falls within or below the range of sand values. In the study location, unique litter categories that differ from other studies have been observed (Bao et al., 2018; Cordova and Nurhati, 2019; Deidun et al., 2018; Duhec et al., 2015; Faizal et al., 2019, 2020; Jakovljevic et al., 2020; Maharjan et al., 2022; Moy et al., 2018; Papakonstantinou et al., 2021, 2021; Suteja et al., 2021). It should be noted that these litter categories are greatly influenced by local habits and culture (Carmi 2019; Kiessling et al., 2017; Liu et al., 2013; Mecho et al., 2021; Williams et al., 2016). In this location near the river mouth, there is wood stranded from upstream events; these events are also one of the study challenges in this location.

CONCLUSIONS

This study aimed to develop a comprehensive beach litter monitoring system by integrating UAV and GIS. The UAV was used by a small-UAV, it offers several advantages, including extensive coverage and high-detail data collection as needed. This method presents a viable alternative for enhancing beach litter monitoring efforts. In this study, the classification of litter reflectance was achieved through the box-plot method, which involved analyzing the reflectance values of each category, to establish accurate threshold values. By employing GIS, the delineated areas with litter and non-litter areas based on the threshold values were conducted. To ensure reliability and validity, the Slovin’s Formula was utilized to determine the required total sample for validation purposes. This proposed monitoring system is user-friendly as it only requires one person and effectively captures dominant forms

of litter, which are plastic bags with white color and styrofoam. Additionally, this study proposed calculating abundance using percentage measurements within square-meter areas.

Inconsequential, this approach still has limitations and requires refinement, particularly in the reflectance value interval, which is covered by sand reflectance values. Notably, local customs and culture have a significant impact on litter classifications. The study area is near the river mouth, and there is timber stranded from upstream occurrences, which is also one of the study's obstacles. Moving forward, there are two main tasks to address given the complexity of objects in the images: enhancing image sharpness through preprocessing techniques such as super-resolution methods and implementing deep learning methods like pixel-wise or semantic segmentation for object classification at a pixel level. Last but not least, improving these results by using spectral cameras installed on UAVs.

Acknowledgment

I would like to thank Josaphat Microwave Remote Sensing Laboratory, Center for Environmental Remote Sensing, Chiba University (Prof. Josaphat Tetuko Sri Sumantyo, Ph.D) for his facility during processing data.

REFERENCES

1. Aber, J.S., Marzloff, I., Ries, J.B., Aber, S.E.W. 2019. Small-format aerial photography and UAS imagery (Second Edi). Elsevier. <https://doi.org/10.1016/C2016-0-03506-4>
2. Anadkat, A.P., Monisha, B.V, Puthineedi, M., Patnaik, A.K., Shekhar, R., Syed, R. Drone based solid waste detection using deep learning & image processing. In: Alliance International Conference on Artificial Intelligence and Machine Learning (AICAAM), April 2019, 357–364.
3. Andriolo, U., Garcia-Garin, O., Vighi, M., Borrell, A., Gonçalves, G. 2022. Beached and Floating litter surveys by unmanned aerial vehicles: operational analogies and differences. *Remote Sensing*, 14(6), 1336. <https://doi.org/10.3390/rs14061336>
4. Andriolo, U., Gonçalves, G., Rangel-Buitrago, N., Paterni, M., Bessa, F., Gonçalves, L. M.S., Sobral, P., Bini, M., Duarte, D., Fontán-Bouzas, Á., Gonçalves, D., Kataoka, T., Luppichini, M., Pinto, L., Topouzelis, K., Vélez-Mendoza, A., Merlino, S. 2021. Drones for litter mapping: an inter-operator concordance test in marking beached items on aerial images. *Marine Pollution Bulletin*, 169, 112542. <https://doi.org/10.1016/j.marpolbul.2021.112542>
5. Andriolo, U., Gonçalves, G., Sobral, P., Fontán-Bouzas, Á., Bessa, F. 2020. Beach-dune morphodynamics and marine macro-litter abundance: An integrated approach with unmanned aerial System. *Science of the Total Environment*, 749, 141474. <https://doi.org/10.1016/j.scitotenv.2020.141474>
6. Argeswara, J., Hendrawan, I.G., Dharma, I.G.B.S., Germanov, E. 2021. What's in the soup? Visual characterization and polymer analysis of microplastics from an Indonesian manta ray feeding ground. *Marine Pollution Bulletin*, 168, 112427. <https://doi.org/10.1016/j.marpolbul.2021.112427>
7. Bak, S.H., Hwang, D.H., Kim, H.M., Yoon, H.J., Hwang, D.H., Kim, H.M., Yoon, H.J. 2019. Detection and monitoring of beach litter using uav image and deep neural network. *International Archives of the Photogrammetry, Remote Sensing and Spatial Information Sciences*, XLII-3/W8, 55–58. <https://doi.org/10.5194/isprs-archives-XLII-3-W8-55-2019>
8. Bali Partnership. 2019. Solving waste management issues together. <https://www.balipartnership.org/>
9. Bao, Z., Sha, J., Li, X., Hanchiso, T., Shifaw, E. 2018. Monitoring of beach litter by automatic interpretation of unmanned aerial vehicle images using the segmentation threshold method. *Marine Pollution Bulletin*, 137(July), 388–398. <https://doi.org/10.1016/j.marpolbul.2018.08.009>
10. Carmi, N. 2019. On social distress, littering and nature conservation: the case of Jisr A-Zarka. *Coastal Management*, 47(4), 347–361. <https://doi.org/10.1080/08920753.2019.1598223>
11. CNN Indonesia. 2021. The Environment and Forestry Service Transports 1,150 tons of garbage from the beach in badung, Bali. <https://www.cnnindonesia.com/nasional/20211231045143-20-740842/dlhk-angkut-1150-ton-sampah-kiriman-dari-pantai-di-badung-bali>
12. Conley, G., Zinn, S.C., Hanson, T., McDonald, K., Beck, N., Wen, H. 2022. Using a deep learning model to quantify trash accumulation for cleaner urban stormwater. *Computers, Environment and Urban Systems*, 93, 101752. <https://doi.org/10.1016/j.compenvurbsys.2021.101752>
13. Cordova, M.R., Iskandar, M.R., Muhtadi, A., Nurhasanah, Saville, R., Riani, E. 2022. Spatio-temporal variation and seasonal dynamics of stranded beach anthropogenic debris on Indonesian beach from the results of nationwide monitoring. *Marine Pollution Bulletin*, 182, 114035. <https://doi.org/10.1016/j.marpolbul.2022.114035>
14. Cordova, M.R., Nurhati, I. S. 2019. Major sources and monthly variations in the release of land-derived marine debris from the Greater Jakarta area, Indonesia. *Scientific Reports*, 9(1), 18730. <https://doi.org/10.1038/s41598-019-41873-0>

- doi.org/10.1038/s41598-019-55065-2
15. Cózar, A., Aliani, S., Basurko, O.C., Arias, M., Isobe, A., Topouzelis, K., Rubio, A., Morales-Caselles, C. 2021. Marine Litter Windrows: A Strategic Target to Understand and Manage the Ocean Plastic Pollution. *Frontiers in Marine Science*, 8(February), 1–9. <https://doi.org/10.3389/fmars.2021.571796>
 16. Deidun, A., Gauci, A., Lagorio, S., Galgani, F. 2018. Optimising beached litter monitoring protocols through aerial imagery. *Marine Pollution Bulletin*, 131(February), 212–217. <https://doi.org/10.1016/j.marpolbul.2018.04.033>
 17. Directorate of Waste Management Directorate General of Waste and B3 Management Minister of Environment and Forestry. 2020. Achievement of Waste Management Performance. <https://sipsn.menlhk.go.id/sipsn/>
 18. Duhec, A.V., Jeanne, R.F., Maximenko, N., Hafner, J. 2015. Composition and potential origin of marine debris stranded in the western indian ocean on remote Alphonse Island, Seychelles. *Marine Pollution Bulletin*, 96(1–2), 76–86. <https://doi.org/10.1016/j.marpolbul.2015.05.042>
 19. Faizal, A., Samad, W., Werorilangi, S. 2019. Visible reflectance characteristics of marine debris in the sandy beach. *Journal of Physics: Conference Series*, 1341(2), 022011. <https://doi.org/10.1088/1742-6596/1341/2/022011>
 20. Faizal, A., Werorilangi, S., Samad, W. 2020. Spectral characteristics of plastic debris in the beach: case study of Makassar coastal area. *Indonesian Journal of Geography*, 52(1), 8–14. <https://doi.org/10.22146/ijg.40519>
 21. Freitas, S., Silva, H., Silva, E. 2021. Remote hyperspectral imaging acquisition and characterization for marine litter detection. *Remote Sensing*, 13(13), 1–22. <https://doi.org/10.3390/rs13132536>
 22. Garcia-Garin, O., Monleón-Getino, T., López-Brosa, P., Borrell, A., Aguilar, A., Borja-Robalino, R., Cardona, L., Vighi, M. 2021. Automatic detection and quantification of floating marine macro-litter in aerial images: Introducing a novel deep learning approach connected to a web application in R. *Environmental Pollution*, 273, 116490. <https://doi.org/10.1016/j.envpol.2021.116490>
 23. García-Rivera, S., Lizaso, J.L.S., Millán, J.M.B. 2018. Spatial and temporal trends of marine litter in the Spanish Mediterranean seafloor. *Marine Pollution Bulletin*, 137, 252–261. <https://doi.org/10.1016/j.marpolbul.2018.09.051>
 24. Geraeds, M., van Emmerik, T., de Vries, R., bin Ab Razak, M. S. 2019. Riverine Plastic Litter Monitoring Using Unmanned Aerial Vehicles (UAVs). *Remote Sensing*, 11(17), 2045. <https://doi.org/10.3390/rs11172045>
 25. Goddijn-Murphy, L., Peters, S., van Sebille, E., James, N.A., Gibb, S. 2018. Concept for a hyperspectral remote sensing algorithm for floating marine macro plastics. *Marine Pollution Bulletin*, 126(October 2017), 255–262. <https://doi.org/10.1016/j.marpolbul.2017.11.011>
 26. Goddijn-Murphy, L., Williamson, B. J., McIlvenny, J., Corradi, P., Goddijn-murphy, L., Williamson, B. J., McIlvenny, J., Corradi, P. 2022. Using a UAV Thermal Infrared Camera for Monitoring Floating Marine Plastic Litter. *Remote Sensing*, 14(13), 3179. <https://doi.org/10.3390/rs14133179>
 27. Gonçalves, G., Andriolo, U., Gonçalves, L.M.S., Sobral, P., Bessa, F. 2022. Beach litter survey by drones: Mini-review and discussion of a potential standardization. *Environmental Pollution*, 315(September), 120370. <https://doi.org/10.1016/j.envpol.2022.120370>
 28. Gonçalves, G., Andriolo, U., Gonçalves, L., Sobral, P., Bessa, F. 2020. Quantifying Marine Macro Litter Abundance on a Sandy Beach Using Unmanned Aerial Systems and Object-Oriented Machine Learning Methods. *Remote Sensing*, 12(16), 1–19. <https://doi.org/10.3390/rs12162599>
 29. Gonçalves, G., Andriolo, U., Pinto, L., Bessa, F. 2020. Mapping marine litter using UAS on a beach-dune system: a multidisciplinary approach. *Science of The Total Environment*, 706, 135742. <https://doi.org/10.1016/j.scitotenv.2019.135742>
 30. González-Fernández, D., Hanke, G. 2017. Toward a Harmonized Approach for Monitoring of Riverine Floating Macro Litter Inputs to the Marine Environment. *Frontiers in Marine Science*, 4. <https://doi.org/10.3389/fmars.2017.00086>
 31. González, D., Hanke, G., Tweehuysen, G., Bellert, B., Holzhauer, M., Palatinus, A., Hohenblum, P., Oosterbaan, L. 2016. Riverine Litter Monitoring - Options and Recommendations - Thematic Report. In JRC Scientific and Technical Reports (Issue February). <https://doi.org/10.2788/461233>
 32. Grelaud, M., Ziveri, P. 2020. The generation of marine litter in Mediterranean island beaches as an effect of tourism and its mitigation. *Scientific Reports*, 10(1), 20326. <https://doi.org/10.1038/s41598-020-77225-5>
 33. Gunawan, H., Yeny, I., Karlina, E., Suharti, S., Murniati, Subarudi, Mulyanto, B., Ekawati, S., Garsestiasih, R., Pratiwi, Sumirat, B. K., Sawitri, R., Heriyanto, N. M., Takandjandji, M., Widarti, A., Surati, Desmiwati, Kalima, T., Effendi, R., Nurlia, A. 2022. Integrating social forestry and biodiversity conservation in Indonesia. *Forests*, 13(12), 2152. <https://doi.org/10.3390/f13122152>
 34. Hajar, N. R. 2019. The Potential Effects of Marine Litter on Tourism at Kuta Beach, Bali : A systemic analysis.
 35. Hardesty, B.D., Roman, L., Leonard, G.H., Mallos, N., Pragnell-Raasch, H., Campbell, I., Wilcox, C.

2021. Socioeconomics effects on global hotspots of common debris items on land and the seafloor. *Global Environmental Change*, 71, 102360. <https://doi.org/10.1016/j.gloenvcha.2021.102360>
36. Haseler, M., Schernewski, G., Balciunas, A., Sabaliauskaite, V. 2018. Monitoring methods for large micro- and meso-litter and applications at Baltic beaches. *Journal of Coastal Conservation*, 22(1), 27–50. <https://doi.org/10.1007/s11852-017-0497-5>
37. Jakovljevic, G., Govedarica, M., Alvarez-Taboada, F. 2020. A Deep Learning Model for Automatic Plastic Mapping Using Unmanned Aerial Vehicle (UAV) Data. *Remote Sensing*, 12(9), 1515. <https://doi.org/10.3390/rs12091515>
38. Kako, S., Isobe, A., Magome, S. 2012. Low altitude remote-sensing method to monitor marine and beach litter of various colors using a balloon equipped with a digital camera. *Marine Pollution Bulletin*, 64(6), 1156–1162. <https://doi.org/10.1016/j.marpolbul.2012.03.024>
39. Kiessling, T., Salas, S., Mutafoğlu, K., Thiel, M. 2017. Who cares about dirty beaches? Evaluating environmental awareness and action on coastal litter in Chile. *Ocean and Coastal Management*, 137, 82–95. <https://doi.org/10.1016/j.ocecoaman.2016.11.029>
40. Kikaki, A., Karantzalos, K., Power, C.A., Raitsos, D.E. 2020. Remotely sensing the source and transport of marine plastic debris in bay islands of Honduras (Caribbean Sea). *Remote Sensing*, 12(11), 1727. <https://doi.org/10.3390/rs12111727>
41. Kraft, M., Piechocki, M., Ptak, B., Walas, K. 2021. Autonomous, onboard vision-based trash and litter detection in low altitude aerial images collected by an unmanned aerial vehicle. *Remote Sensing*, 13(5), 965. <https://doi.org/10.3390/rs13050965>
42. Kylili, K., Kyriakides, I., Artusi, A., Hadjistassou, C. 2019. Identifying floating plastic marine debris using a deep learning approach. *Environmental Science and Pollution Research*, 26(17), 17091–17099. <https://doi.org/10.1007/s11356-019-05148-4>
43. Lam, T. W.L., Fok, L., Ma, A.T.H., Li, H.-X., Xu, X.-R., Cheung, L.T.O., Wong, M.H. 2022. Microplastic contamination in marine-cultured fish from the Pearl River Estuary, South China. *Science of The Total Environment*, 827, 154281. <https://doi.org/10.1016/j.scitotenv.2022.154281>
44. Lebreton, L.C.M., Greer, S.D., Borrero, J.C. 2012. Numerical modelling of floating debris in the world's oceans. *Marine Pollution Bulletin*, 64(3), 653–661. <https://doi.org/10.1016/j.marpolbul.2011.10.027>
45. Leslie, H.A., van Velzen, M.J.M., Brandsma, S.H., Vethaak, A.D., Garcia-Vallejo, J.J., Lamoree, M.H. 2022. Discovery and quantification of plastic particle pollution in human blood. *Environment International*, 107199. <https://doi.org/10.1016/j.envint.2022.107199>
46. Lestari, P., Trihadiningrum, Y. 2019. The impact of improper solid waste management to plastic pollution in Indonesian coast and marine environment. *Marine Pollution Bulletin*, 149, 110505. <https://doi.org/10.1016/j.marpolbul.2019.110505>
47. Liro, M., Emmerik, T. van, Wyzga, B., Liro, J., Mikuś, P. 2020. Macroplastic storage and remobilization in rivers. *Water*, 12(7), 2055. <https://doi.org/10.3390/w12072055>
48. Liu, T.K., Wang, M.W., Chen, P. 2013. Influence of waste management policy on the characteristics of beach litter in Kaohsiung, Taiwan. *Marine Pollution Bulletin*, 72(1), 99–106. <https://doi.org/10.1016/j.marpolbul.2013.04.015>
49. Lo, H.-S., Wong, L.-C., Kwok, S.-H., Lee, Y.-K., Po, B. H.-K., Wong, C.-Y., Tam, N. F.-Y., Cheung, S.-G. 2020. Field test of beach litter assessment by commercial aerial drone. *Marine pollution bulletin*, 151, 110823. <https://doi.org/10.1016/j.marpolbul.2019.110823>
50. Maharjan, N., Miyazaki, H., Pati, B.M., Dailey, M.N., Shrestha, S., Nakamura, T. 2022. Detection of river plastic using uav sensor data and deep learning. *remote sensing*, 14(13). <https://doi.org/10.3390/rs14133049>
51. Mandal, K., Dey, P. 2022. Coastal vulnerability analysis and RIDIT scoring of socio-economic vulnerability indicators – A case of Jagatsinghpur, Odisha. *International Journal of Disaster Risk Reduction*, 79, 103143. <https://doi.org/10.1016/j.ijdr.2022.103143>
52. Mandirola, M., Casarotti, C., Peloso, S., Lanese, I., Brunesi, E., Senaldi, I., Risi, F., Monti, A., Facchetti, C. 2021. Guidelines for the use of Unmanned Aerial Systems for fast photogrammetry-oriented mapping in emergency response scenarios. *International Journal of Disaster Risk Reduction*, 58, 102207. <https://doi.org/10.1016/j.ijdr.2021.102207>
53. Martin, C., Parkes, S., Zhang, Q., Zhang, X., McCabe, M.F., Duarte, C.M. 2018. Use of unmanned aerial vehicles for efficient beach litter monitoring. *Marine Pollution Bulletin*, 131, 662–673. <https://doi.org/10.1016/j.marpolbul.2018.04.045>
54. Mauludy, M.S., Yunanto, A., Yona, D. 2019. Microplastic Abundances in the Sediment of Coastal Beaches in Badung, Bali. *Jurnal Perikanan Universitas Gadjah Mada*, 21(2), 73. <https://doi.org/10.22146/jfs.45871>
55. Maximenko, N., Corradi, P., Law, K.L., Seville, E. Van, Garaba, S.P., Lampitt, R.S., Galgani, F., Martinez-Vicente, V., Goddijn-Murphy, L., Veiga, J.M., Thompson, R.C., Maes, C., Moller, D., Löscher, C.R., Addamo, A.M., Lamson, M.R., Centurioni, L.R., Posth, N.R., Lumpkin, R., Wilcox, C. 2019. Towards the integrated marine debris observing system. *Frontiers in Marine Science*, 6. <https://doi.org/10.3389/fmars.2019.00000>

- org/10.3389/fmars.2019.00447
56. Mecho, A., Sellanes, J., Aguzzi, J. 2021. Seafloor litter at oceanic islands and seamounts of the southeastern Pacific. *Marine Pollution Bulletin*, 170, 112641. <https://doi.org/10.1016/j.marpolbul.2021.112641>
 57. Meijer, L.J.J., van Emmerik, T., van der Ent, R., Schmidt, C., Lebreton, L. 2021. More than 1000 rivers account for 80% of global riverine plastic emissions into the ocean. *Science Advances*, 7(18), 1–14. <https://doi.org/10.1126/sciadv.aaz5803>
 58. Merlino, S., Paterni, M., Berton, A., Massetti, L. 2020. Unmanned Aerial Vehicles for Debris Survey in Coastal Areas: Long-Term Monitoring Programme to Study Spatial and Temporal Accumulation of the Dynamics of Beached Marine Litter. *Remote Sensing*, 12(8), 1260. <https://doi.org/10.3390/rs12081260>
 59. Merlino, S., Paterni, M., Locritani, M., Andriolo, U., Gonçalves, G., Massetti, L. 2021. Citizen science for marine litter detection and classification on unmanned aerial vehicle images. *Water*, 13(23), 3349. <https://doi.org/10.3390/w13233349>
 60. Miladinova, S., Macias, D., Stips, A., Garcia-Gorritz, E. 2020. Identifying distribution and accumulation patterns of floating marine debris in the Black Sea. *Marine Pollution Bulletin*, 153, 110964. <https://doi.org/10.1016/j.marpolbul.2020.110964>
 61. Moy, K., Neilson, B., Chung, A., Meadows, A., Castrence, M., Ambagis, S., Davidson, K. 2018. Mapping coastal marine debris using aerial imagery and spatial analysis. *Marine Pollution Bulletin*, 132, 52–59. <https://doi.org/10.1016/j.marpolbul.2017.11.045>
 62. Muhajir, A. 2019. This is the latest data and sources of garbage in Bali. In Mongabay. <https://www.mongabay.co.id/2019/07/02/inilah-data-dan-sumber-sampah-terbaru-di-bali/>
 63. Nazerdeylami, A., Majidi, B., Movaghar, A. 2021. Autonomous litter surveying and human activity monitoring for governance intelligence in coastal eco-cyber-physical systems. *Ocean & Coastal Management*, 200, 105478. <https://doi.org/10.1016/j.ocecoaman.2020.105478>
 64. Over, J.-S.R., Ritchie, A.C., Kranenburg, C.J., Brown, J.A., Buscombe, D.D., Noble, T., Sherwood, C.R., Warrick, J.A., Wernette, P.A., Jenna A., Buscombe, D.D., Noble, T., Sherwood, C.R., Warrick, J.A., Wernette, P.A. 2021. Processing coastal imagery with Agisoft Metashape Professional Edition, version 1.6—Structure from motion workflow documentation. In U.S. Geological Survey Open-File Report 2021–1039. <https://doi.org/10.3133/ofr20211039>
 65. Papakonstantinou, A., Batsaris, M., Spondylidis, S., Topouzelis, K. 2021. A citizen science unmanned aerial system data acquisition protocol and deep learning techniques for the automatic detection and mapping of marine litter concentrations in the coastal zone. *Drones*, 5(1), 1–21. <https://doi.org/10.3390/drones5010006>
 66. Phelan, A.A., Ross, H., Setianto, N.A., Fielding, K., Pradipta, L. 2020. Ocean plastic crisis—mental models of plastic pollution from remote Indonesian coastal communities. *PLOS ONE*, 15(7), e0236149. <https://doi.org/10.1371/journal.pone.0236149>
 67. Pinto, L., Andriolo, U., Gonçalves, G. 2021. Detecting stranded macro-litter categories on drone orthophoto by a multi-class Neural Network. *Marine Pollution Bulletin*, 169(16), 112594. <https://doi.org/10.1016/j.marpolbul.2021.112594>
 68. Rochwulaningsih, Y., Sulistiyono, S.T., Masruroh, N.N., Maulany, N.N. 2019. Marine policy basis of Indonesia as a maritime state: The importance of integrated economy. *Marine Policy*, 108, 103602. <https://doi.org/10.1016/j.marpol.2019.103602>
 69. Sakti, A.D., Sembiring, E., Rohayani, P., Fauzan, K.N., Anggraini, S., Santoso, C., Patricia, V.A., Titon, K., Ihsan, N., Ramadan, A. H., Arjakusuma, S., Candra, D. S. 2023. Identification of Illegally Dumped Plastic Waste in a Highly Polluted River in Indonesia Using Sentinel-2 Satellite Imagery. *Scientific Reports*, 1–16. <https://doi.org/10.1038/s41598-023-32087-5>
 70. Schuyler, Q., Willis, K., Lawson, T.J., Mann, V., Wilcox, C., Hardesty, B.D. 2020. Handbook of Survey Methodology - Plastics Leakage. CSIRO, Australia, EP178700, 1–47.
 71. Secretariat of the Convention on Biological Diversity 2016. Marine Debris: Understanding, Preventing and Mitigating the Significant Adverse Impacts on Marine and Coastal Biodiversity. In CBD Technical Series, 83. <https://www.cbd.int/doc/publications/cbd-ts-83-en.pdf>
 72. Serafino, F., Bianco, A. 2021. Use of X-Band Radars to Monitor Small Garbage Islands. *Remote Sensing*, 13(18), 3558. <https://doi.org/10.3390/rs13183558>
 73. Suteja, Y., Atmadipoera, A.S., Riani, E., Nurjaya, I.W., Nugroho, D., Purwiyanto, A.I.S. 2021. Stranded marine debris on the touristic beaches in the south of Bali Island, Indonesia: The spatiotemporal abundance and characteristic. *Marine Pollution Bulletin*, 173(PA), 113026. <https://doi.org/10.1016/j.marpolbul.2021.113026>
 74. Topouzelis, K., Papageorgiou, D., Karagaitanakis, A., Papakonstantinou, A., Ballesteros, M.A. 2020. Remote sensing of sea surface artificial floating plastic targets with Sentinel-2 and unmanned aerial systems (plastic litter project 2019). *Remote Sensing*, 12(12). <https://doi.org/10.3390/rs12122013>
 75. Topouzelis, K., Papakonstantinou, A., Garaba, S.P. 2019. Detection of floating plastics from satellite and unmanned aerial systems (Plastic Litter Project 2018). *International Journal of Applied Earth*

- Observation and Geoinformation, 79, 175–183. <https://doi.org/10.1016/j.jag.2019.03.011>
76. van Emmerik, T., Roebroek, C., de Winter, W., Vriend, P., Boonstra, M., Hougee, M. 2020. Riverbank macrolitter in the Dutch Rhine–Meuse delta. *Environmental Research Letters*, 15(10), 104087. <https://doi.org/10.1088/1748-9326/abb2c6>
77. van Emmerik, T., Schwarz, A. 2020. Plastic debris in rivers. *WIREs Water*, 7(1), 1–24. <https://doi.org/10.1002/wat2.1398>
78. van Emmerik, T., Seibert, J., Strobl, B., Etter, S., den Oudendammer, T., Rutten, M., bin Ab Razak, M. S., van Meerveld, I. 2020. Crowd-Based Observations of Riverine Macroplastic Pollution. *Frontiers in Earth Science*, 8. <https://doi.org/10.3389/feart.2020.00298>
79. van Lieshout, C., van Oeveren, K., van Emmerik, T., Postma, E. 2020. Automated River Plastic Monitoring Using Deep Learning and Cameras. *Earth and Space Science*, 7(8). <https://doi.org/10.1029/2019EA000960>
80. Veiga, J.M., Fleet, D., Kinsey, S., Nilsson, P., Vlachogianni, T., Werner, S., Galgani, F., Thompson, R.C., Dagevos, J., Gago, J., Sobral, P., Cronin, R. 2016. JRC Technical Report -Identifying Sources of Marine Litter. <https://doi.org/10.2788/018068>
81. Vriend, P., Roebroek, C.T.J., van Emmerik, T. 2020. Same but different: a framework to design and compare riverbank plastic monitoring strategies. *frontiers. Water*, 2. <https://doi.org/10.3389/frwa.2020.563791>
82. Wang, P., Li, X., Tang, J., Yang, J., Ma, Y., Wu, D., Huo, Z. 2023. Determining the critical threshold of meteorological heat damage to tea plants based on MODIS LST products for tea planting areas in China. *Ecological Informatics*, 77, 102235. <https://doi.org/10.1016/j.ecoinf.2023.102235>
83. Williams, A.T., Rangel-Buitrago, N.G., Anfuso, G., Cervantes, O., Botero, C.M. 2016. Litter impacts on scenery and tourism on the Colombian north Caribbean coast. *Tourism Management*, 55, 209–224. <https://doi.org/10.1016/j.tourman.2016.02.008>
84. Wolf, M., van den Berg, K., Garaba, S.P., Gnann, N., Sattler, K., Stahl, F., Zielinski, O. 2020. Machine learning for aquatic plastic litter detection, classification and quantification (APLastic-Q). *Environmental Research Letters*, 15(11), 114042. <https://doi.org/10.1088/1748-9326/abbd01>
85. Xiao, Y., Dai, S., Xiao, C., Xu, X. 2022. Research and Development of a Real-time UAV Flight Visualization Simulation System. *Journal of Physics: Conference Series*, 2218(1), 012081. <https://doi.org/10.1088/1742-6596/2218/1/012081>
86. Yang, Z., Yu, X., Dedman, S., Rosso, M., Zhu, J., Yang, J., Xia, Y., Tian, Y., Zhang, G., Wang, J. 2022. UAV remote sensing applications in marine monitoring: Knowledge visualization and review. *Science of The Total Environment*, 155939. <https://doi.org/10.1016/j.scitotenv.2022.155939>